

Supplementary Table I: ZIKV-positive tissues by ddPCR and RNAScope

(ZIKV positive tissues were confirmed by detecting viral RNA with ddPCR and RNAScope ZIKV-specific chromogenic probes).

Sample (Necropsy date)	Intravaginal (IVAG) infection				Subcutaneous (sub Q) infection					
	RFc15R (110 dpi)		R1811R (60 dpi)		A12T006 (8 dpi)		RZi15R (21 dpi)		R21612R (21 dpi)	
	PCR	RNAScope	PCR	RNAScope	PCR	RNAScope	PCR	RNAScope	PCR	RNAScope
Lung	-	ND	-	-	-	-	-	ND	-	ND
Spleen	-	ND	-	-	-	-	+	ND	+	ND
Liver	-	ND	-	-	-	-	-	ND	-	ND
Kidney	-	ND	+	+	-	-	+	ND	-	ND
Intestine	-	ND	-	-	-	-	+	ND	-	ND
Stomach	-	ND	-	-	-	-	-	ND	-	ND
Heart	-	ND	+	+	+	+	-	ND	-	ND
Vagina	ND	ND	ND	ND	+	+	-	ND	-	ND
Uterus	-	ND	-	-	+	+	-	ND	-	ND
Inguinal LN	-	ND	+	+	-	-	+	ND	+	ND
Axillary LN	-	ND	-	-	-	-	+	ND	+	ND
Colonic LN	-	ND	+	+	-	-	+	+	+	ND
Mesenteric LN	-	ND	-	-	-	-	+	ND	-	ND
Cervical LN	-	ND	+	+	-	-	-	ND	-	ND
Thoracic SC	-	ND	-	-	-	-	-	ND	-	ND
Cervical SC	-	ND	-	-	-	-	-	ND	-	ND
Lumbar SC	ND	ND	ND	ND	+	+	-	ND	-	ND
Peripheral SC	-	ND	-	-	-	-	+	ND	-	ND
Retina	-	ND	-	-	-	-	-	ND	-	ND
Subventricular zone	-	ND	-	-	-	-	-	ND	-	ND
Hippocampus	-	ND	+	+	-	-	-	ND	-	ND
Frontal lobe cortex	-	ND	-	-	-	-	-	ND	+	ND
Parietal lobe cortex	-	ND	-	-	+	+	-	ND	-	ND
Temporal lobe cortex	-	ND	-	-	-	-	-	ND	-	ND
Occipital lobe cortex	-	ND	-	-	-	-	-	ND	-	ND
Hypothalamus	-	ND	-	-	+	+	-	ND	-	ND
Cerebellum	-	ND	-	-	-	-	+	+	-	ND
Amygdala	-	ND	-	-	+	-	-	ND	-	ND
Caudate nucleus	-	ND	+	-	+	+	-	ND	+	ND

PCR: ddPCR, -: PCR amplification or RNAScope negative, +: PCR amplification or RNAScope positive

MONOCYTE AND DENDRITIC CELL GATING STRATEGY

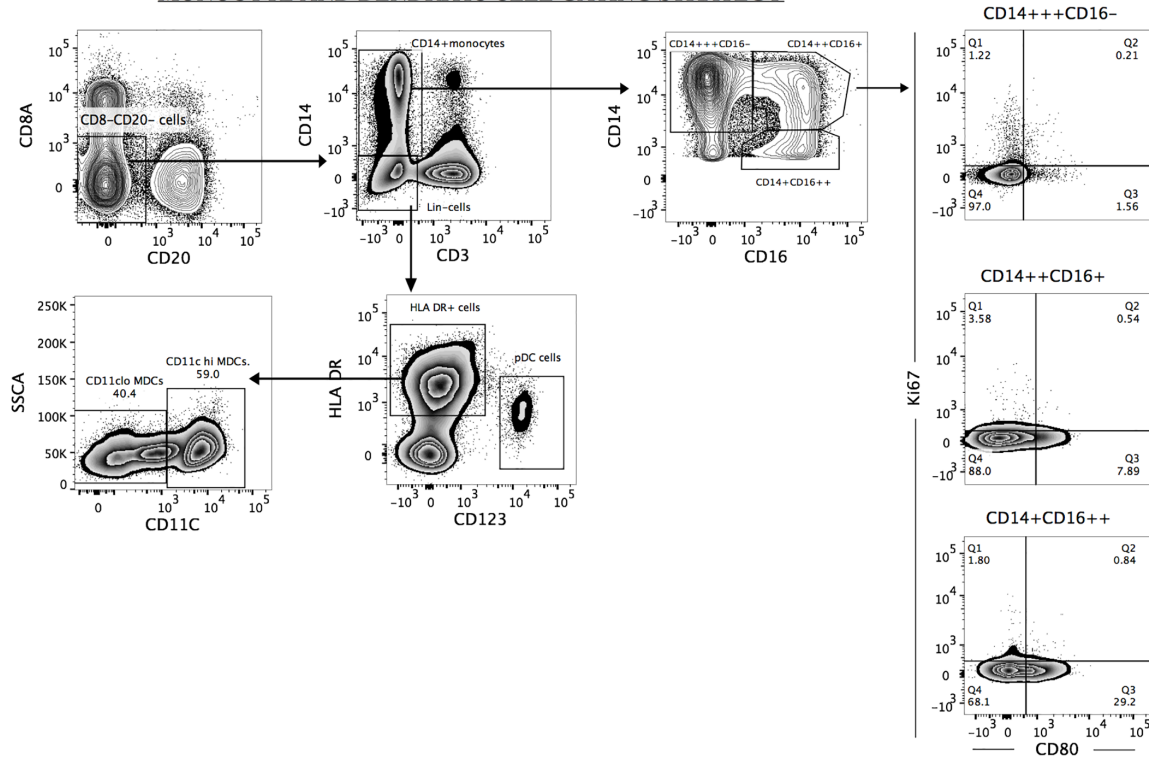


Fig S1. Monocyte and dendritic cell gating strategy: This involved the exclusion of B cells and NK (CD3-CD8 α +) cells from the CD3- population (CD8-CD20-). From the CD8-CD20- population, we gated out CD14+ cells, which were further discriminated into CD14+++CD16- (classical), CD14++CD16+ (intermediate) and CD14+CD16++ (non-classical) monocyte phenotypes. These diverse monocyte phenotypes were further evaluated for their expression of Ki67+ and CD80+ based on the placement of FMO gates. On the other hand, dendritic cells (DCs) were obtained from the Lin- (CD3-, CD8-, CD14- and CD20-) population. From the Lin- population, HLA DR+ cells were excluded and further divided into CD11C hi MDCs and CD11C lo MDCs. We focused on changes that occur in CD11C hi MDCs.

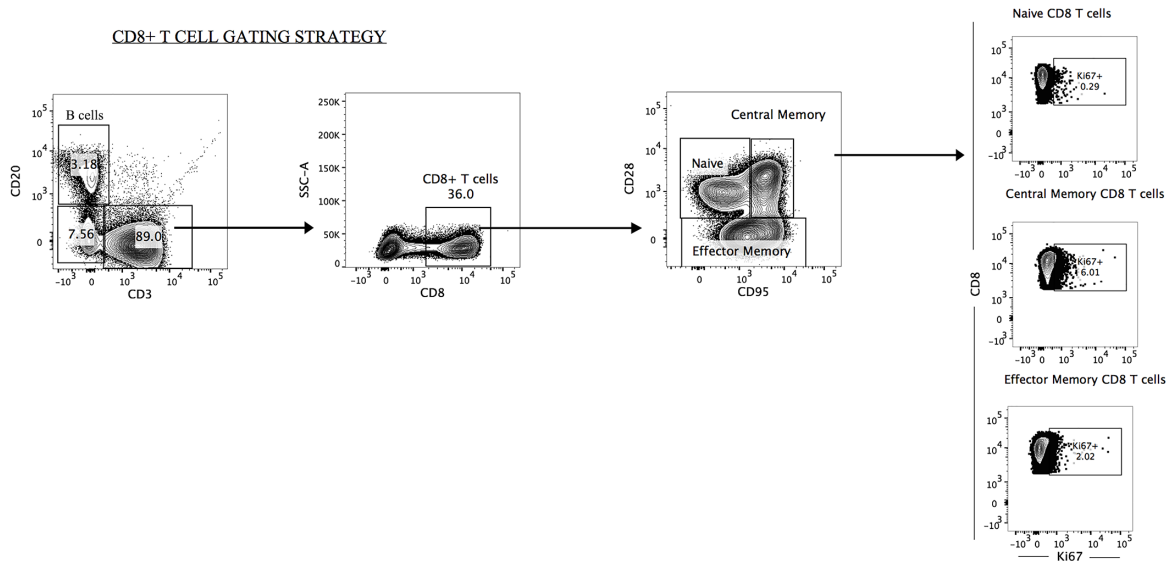


Fig S2. B cell and CD8+ gating strategy. Briefly, B cells were classified as CD3-CD20+ cells. Changes that occurred in these cell frequencies were studied across all experimental animals at diverse time points. From the CD3+ population, we delineated CD8+ T cells and categorized them into respective naive, central memory and effector memory phenotypes. We then focused on Ki67 expression on central memory CD8+ T cells following the placement of an appropriate Fluorescent Minus One (FMO) gate.

NK CELL GATING STRATEGY

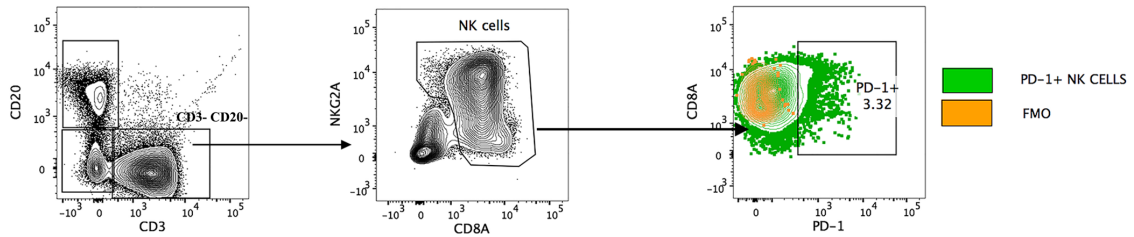


Fig S3. Describing the NK cell gating strategy. From the CD3- population, we obtained NK cells by CD8 α and NKG2A co-expression. Following the placement of a PD-1 FMO gate, we were able to study changes that occur in PD-1+ NK cells during the course of the study.